Failure and Dilatancy Properties of Sand at Relatively Low Stresses

Laurent Lancelot[1]; Isam Shahrour[2]; and Marwan Al Mahmoud[3]

Abstract: Analysis of geotechnical problems concerned by low confinement such as design of shallow foundations and analysis of slope stability and soil liquefaction requires modeling of the soil behavior at low stresses. This note includes a laboratory study of the behavior of Hostun RF sand at low cell pressure (20–50 kPa). Isotropic and triaxial compression drained tests were performed. Drained tests show that both failure and dilatancy angles at low stresses are stress dependent. The contractive/dilative phase transition is observed for loose sand, which may result from the overconsolidated nature of this sand for low values of cell pressure.

DOI: 10.1061/(ASCE)0733-9399(2006)132:12(1396)

CE Database subject headings: Dilatancy; Friction; Localization; Triaxial test; Isotropy; Slope stability; Liquefaction.

Introduction

Modeling the soils behavior at low stresses is of major interest for the design of geotechnical structures concerned by low confinement, such as shallow foundations, slopes, tunnels, and geotechnical structures concerned by either static or cyclic liquefaction. The behavior of granular materials at low stresses presents also a major interest for chemical, pharmaceutical, or food industries concerned by storage and flow problems of powders and granular materials (Lancelot and Shahrour 1994).

The resistance and dilatancy of soils at low stresses was investigated by Ponce and Bell (1971) and Fukushima and Tatsuoka (1984). Triaxial tests performed by Ponce and Bell (1971) show that the decrease in the cell pressure leads to a strong increase in both friction and dilatancy angles. These authors suggest the existence of an apparent cohesion between sand grains at low stresses. This apparent cohesion in sand can also be interpreted with a curved strength envelope suggesting increasing angle of friction at lower stresses. Fukushima and Tatsuoka (1984) observed a small variation in both friction and dilatancy angles for a cell pressure in the range 1–20 kPa; they did not observe cohesion for sand at low stresses.

This note includes a presentation of isotropic and triaxial tests performed on Hostun RF sand at low stresses (20 and 50 kPa). Discussion of experimental results and their comparison with tests performed at conventional cell pressure (50–400 kPa) allow a better understanding of the influence of the confining pressure on the plastic properties of sand, mainly for friction and dilatancy angles.

Experimental Procedure

The determination of mechanical properties of sands at low stresses encounters specific technical problems, mainly for sample preparation and stress and strain measurements. A detailed description of the experimental procedure used in this study is presented in Al Mahmoud (1997). The triaxial testing equipment was fitted with low friction platens, to minimize strain localization during shearing. The force transducer was placed inside the triaxial cell underneath the sample. Cell pressure (respectively, backpressure) was controlled by a digital pressure-volume controller (Menzies 1988) within a 0–2 MPa range (respectively, 0–400 kPa) with 1 kPa resolution (respectively, 0.1 kPa). Sample volume change was measured with a 1 mm^3 resolution using the backpressure controller. Tests were performed with backpressures ranging from 250 to 300 kPa with a Skempton's B parameter greater than 0.96. The extra radial stress due to membrane stiffness was taken into account. Considering membranes as thin elastic cylinders undergoing the same deformations as the sample, the radial extra stress caused by the deforming membrane can be computed as (Fukushima and Tatsuoka 1984)

$$\Delta\sigma_{rm} = \frac{-2E_m t\varepsilon_{\theta m}}{d} \tag{1}$$

where E_m=membrane Young modulus (1.3 MPa); t=membrane thickness (0.2 mm); d=sample diameter (varying during test, initial diameter 70 mm); and $\varepsilon_{\theta m}$=membrane orthoradial strain, supposed equivalent to sample radial strain.

Tests were performed on Hostun RF sand, which is a subangular medium sand (D_{50}=0.471 mm, Cu=2.26, γ_s=25.96 kN/m^3, e_{min}=0.575, and e_{max}=0.943). Samples were prepared by pouring a known mass of air dry sand in the mold, by deposition with a spoon for loose samples, in five lifts each tamped using a steel rammer for dense samples.

[1]Assistant Professor, Laboratoire de Mecanique de Lille (CNRS UMR8107), Ecole Polytechnique Univ. de Lille, Avenue Paul Langevin, 59655 Villeneuve d'Ascq cedex, France.

[2]Professor, Laboratoire de Mecanique de Lille (CNRS UMR8107), Ecole Polytechnique Univ. de Lille, Avenue Paul Langevin, 59655 Villeneuve d'Ascq cedex, France.

[3]Research Fellow, Laboratoire de Mecanique de Lille (CNRS UMR8107), Ecole Polytechnique Univ. de Lille, Avenue Paul Langevin, 59655 Villeneuve d'Ascq cedex, France.

Note. Associate Editor: Ching S. Chang. Discussion open until May 1, 2007. Separate discussions must be submitted for individual papers. To extend the closing date by one month, a written request must be filed with the ASCE Managing Editor. The manuscript for this technical note was submitted for review and possible publication on February 25, 2003; approved on April 27, 2006. This technical note is part of the ***Journal of Engineering Mechanics***, Vol. 132, No. 12, December 1, 2006. ©ASCE, ISSN 0733-9399/2006/12-1396–1399/$25.00.

Table 1. Initial Properties of Tested Samples

Test code	Test type	Initial confining stress σ_0' (kPa)	Initial void ratio e (—)	Relative density I_D (—)
ISO	Isotropically consolidated drained triaxial compression tests	10	0.897	0.124
CID1		20	0.901	0.115
CID2		50	0.884	0.161
CID3		100	0.880	0.171
CID4		200	0.868	0.205
CID5		400	0.852	0.247
CID6		20	0.610	0.904
CID7		50	0.614	0.894
CID8		100	0.614	0.894
FS1	Failure surface test	200	0.895	0.130

Experimental Results

The experimental program included an isotropic compression test, drained triaxial compression tests performed on loose samples at five values of the cell pressure (20, 50, 100, 200, and 400 kPa), triaxial compression tests conducted on dense samples at three values of the cell pressure (20, 50, and 100 kPa) and a particular test performed on a loose sample for the determination of the failure curve. Table 1 summarizes the experimental program; it also provides the initial characteristics of tested samples.

Hydrostatic Compression Test

Results of the hydrostatic compression test carried out on a loose sample (I_D=0.124) are illustrated in Fig. 1. It can be observed that the isotropic normal compression line for loose Hostun sand is reached for relatively high stresses. The slope of this line is equal to C_c=0.115, whereas the slope of the "elastic rebound" line is C_s=0.02. The preconsolidation pressure σ_c' can be estimated to 300 kPa, which means that the sample preparation procedure used in this study leads, even for loose sand, to an overconsolidated material in the low stress range.

Triaxial Compression Tests

Fig. 2 shows triaxial tests conducted on loose (I_D mean value of 0.180) and dense (I_D mean value of 0.897) samples for a cell pressure ranging between 20 and 100 kPa. A stress peak can be observed for dense sand. However no shear band was observed

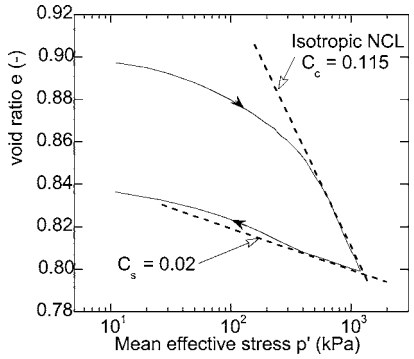

Fig. 1. Isotropic test on loose Hostun RF sand

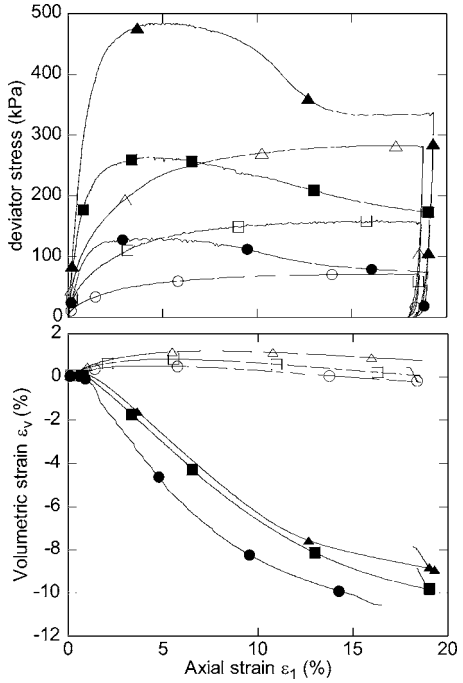

Fig. 2. Drained triaxial tests for Hostun RF sand for confining pressures of 20 kPa (open circle=loose, closed circle=dense), 50 kPa (open square=loose, closed square=dense), and 100 kPa (open triangle=loose, closed triangle=dense)

and sample bulging remained unnoticeable until approximately 8% axial strain. No stress peak occurs for loose samples and bulging appeared even later (10–12% axial strain). A vanishing stiffness can be observed for both loose and dense samples. The evolution of volumetric strain shows a transition between contracting and dilating behavior. It can be seen that loose sand exhibits first a contracting behavior followed by a low dilatation; the latter can be attributed to the sand overconsolidation at this level of stress, as shown on the isotropic test presented in Fig. 1. No constant volume deformation is observed, although for dense samples an inflexion can be noticed in the variation of the volumetric strain for axial strains corresponding roughly to stress peak, indicating a decrease in the sample dilating rate from this state onwards.

Failure and Dilatancy Properties of Hostun Sand at Low Stresses

Angle of Friction and Failure Surface

The fact that the friction angle depends on the confining stress is generally admitted in the literature. Tests conducted by Kolymbas and Wu (1990) on Karlsruhe sand and those carried out on Hostun RF sand show similar trends (Fig. 3). However Fukushima and Tatsuoka (1984) observed on Toyoura sand a low dependency of the friction angle on the cell pressure for confining stresses smaller than 10 kPa.

Lo and Chu (1993) proposed a special testing procedure for a one-test determination of the failure curve. The sample is loaded along a drained path until a state of stress close to the failure surface (deviator stress close to maximum). Then the sample is loaded with an imposed dilation rate in such a way that a pore pressure increase is generated, which induces a decrease in the

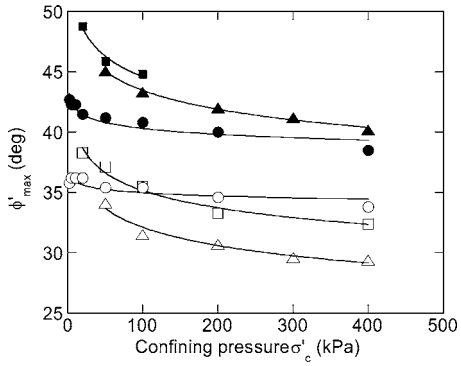

Fig. 3. Influence of confining pressure on maximum friction angle for different sands: Hostun (open square=loose, closed square=dense), Karlsruhe (open triangle=loose, closed triangle =dense), adapted from Kolymbas and Wu, 1990), and Toyoura (open circle=loose, closed circle=dense, adapted from Fukushima and Tatsuoka, 1984)

effective mean pressure p'. The state of stress in the $p'-q$ plane attains the failure surface and subsequently remains on this surface during shearing (see Fig. 4 for test FS1 with 200 kPa initial cell pressure and an imposed dilation rate of -1). In the $p'-q$ plane, the failure line can be traced back from a mean pressure of 200 kPa to virtually 0. Stress paths followed in drained tests on loose sand have been added in Fig. 4 and the points of maximum state of stress show a good agreement with the FS1 curve.

In addition to the fact that the failure curve is nonlinear, it is shown that this curve passes through the origin of the stress axes, which shows the absence of cohesion for sand.

Dilatancy

The dilatancy angle ψ is defined by the relation $\tan(\psi) = -(\delta\varepsilon_v/\delta\varepsilon_1)$. Fig. 5 illustrates the variation of the maximum dilatancy angle (Ψ_{max}) with cell pressure for several sands. It can be observed that ψ_{max} depends both on initial density and cell pressure. For loose sand, a contracting behavior ($\Psi_{max}<0$) is observed for high cell pressures, whereas for low cell pressure a dilating behavior is observed with low values of ψ_{max}. Larger dilatancy values are observed for dense samples with a strong influence on the cell pressure.

According to Rowe (1962) dilatancy can be related to internal friction as follows:

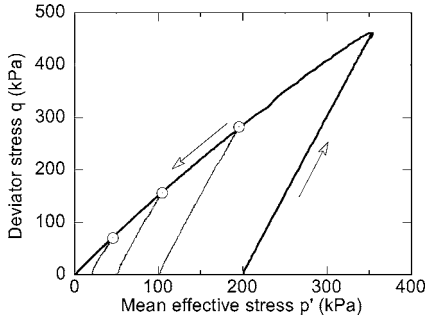

Fig. 4. One-test failure line for loose Hostun RF sand

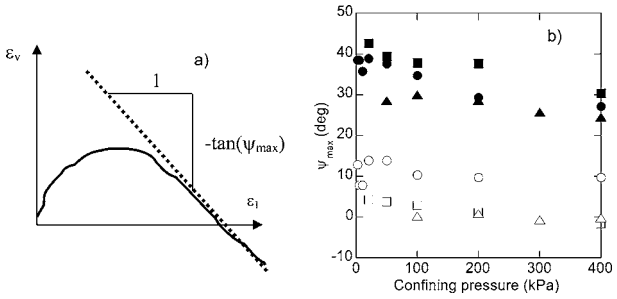

Fig. 5. Influence of confining pressure on ψ_{max} for Hostun sand (open square=loose, closed square=dense), Karlsruhe sand (open triangle=loose, closed triangle=dense, adapted from Kolymbas and Wu 1990) and Toyoura sand (open circle=loose, closed circle=dense, adapted from Fukushima and Tatsuoka 1984)

$$\frac{\sigma'_1}{\sigma'_3} = \left(\frac{\sigma'_1}{\sigma'_3}\right)_c \left[1 - \frac{\partial\varepsilon_v}{\partial\varepsilon_1}\right] \tag{2}$$

where the subscript c means critical (effective stress ratio for a zero dilatancy rate). Fig. 6 shows that for drained tests, the slope of the best fit line is equal to 3.6, corresponding to a critical friction angle $\varphi'_c = 34°$. For quartz sands, a typical value of 33° is reported for the critical friction angle (Bolton 1986). For Hostun RF sand, values between 30 and 32° were reported for φ'_c (Biarez and Ziani 1991 and Konrad et al. 1991). Fig. 6 shows that the ultimate stress states for tests conducted at low cell pressures lie above the best fit line. However this apparent stress dependency of φ'_c can actually be the consequence of postfailure strain localization, which for a given initial density is more likely to occur for low confining pressures.

Critical State

The critical state theory stipulates that for large strains, the state of a soil element tends toward a unique surface in a void ratio e—mean pressure p'—deviator stress q space, called the critical state surface (Roscoe et al. 1958).

Fig. 7 shows results of triaxial drained tests in the $e-\log(p')$ diagram (dots designate ultimate states). Ultimate states for tests CID3–CID5 (conventional confining stresses 100–400 kPa) fall on a line almost parallel to the normal compression line (NCL) obtained in isotropic test. Note that Biarez and Hicher (1994), based on many tests on various sands, propose as an approximate

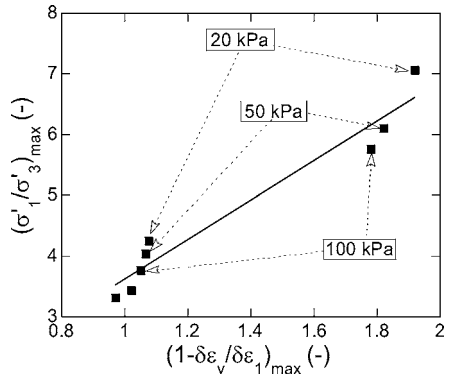

Fig. 6. Rowe's relationship (1962) between dilatancy and internal friction in Hostun RF sand at low pressures

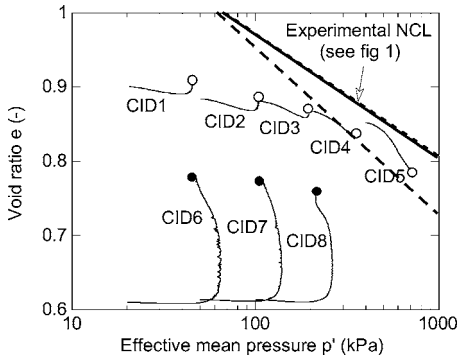

Fig. 7. End points for low stress tests, relative to normal consolidation line. Dashed line=approximate location of critical state line adapted from Biarez and Hicher (1994).

location for the critical state line the line passing through the points (0.1 MPa, e_{max}) and (50 MPa, e_{min}), which is represented as a dashed line on Fig. 7. Tests CID3–CID5 end up close to this line. However it is observed that the distance from ultimate states to the NCL increases with the decrease in cell pressure and the augmentation of sand density. It can be admitted (e.g., Biarez and Hicher 1994) that if the line joining the ultimate states is not parallel to NCL, these points do not correspond to critical state, probably because of strain localization. As this situation is indeed observed in Fig. 7, no conclusion should be drawn for critical state at low stresses from the present data.

Conclusion

This note included an experimental study of the behavior of Hostun RF sand at low stresses (20–50 kPa). It provides valuable data for the calibration of constitutive relations at low stresses. Comparison of tests performed at low stresses with those conducted at conventional stresses (100–400 kPa) shows that at low stresses, the friction and dilatancy angles are stress dependent. A contracting/dilating behavior is observed even for loose sand, which may result from the overconsolidation nature of samples tested at low stresses.

Notation

The following symbols are used in this technical note:

B = Skempton's parameter;
C_c = sand compression index;
C_s = sand swelling index;
E_m = rubber membrane Young modulus;
e = void ratio;
I_D = density index;
p' = $(\sigma'_1+2\sigma'_3)/3$; mean effective stress;
q = $\sigma'_1-\sigma'_3$; deviator stress;
t = rubber membrane thickness;
$\Delta\sigma_{rm}$ = extra radial stress due to membrane stiffness;
ε_1 = axial strain;
ε_v = volumic strain;
$\varepsilon_{\theta m}$ = membrane orthoradial strain;
σ'_c = effective consolidation stress;
σ'_0 = effective confining stress;
σ'_1 = major principal stress; axial stress;
σ'_3 = minor principal stress; radial stress;
φ' = internal angle of friction;
φ'_{cv} = internal angle of friction at constant volume;
φ'_c = internal angle of friction at critical state;
φ'_{lim} = large strain internal angle of friction;
φ'_{max} = peak internal angle of friction;
ψ = dilatancy angle; and
ψ_{max} = dilatancy angle for peak deviator stress.

Subscripts

c = critical, corresponds to zero dilatancy rate.

References

Al Mahmoud, M. (1997). "Etude en laboratoire du comportement des sables sous faibles contraintes." Ph.D. dissertation, Univ. of Lille, France.

Biarez, J., and Hicher, P.-Y. (1994). *Elementary mechanics of soil behaviour*, Balkema, Rotterdam, The Netherlands.

Biarez, J., and Ziani, F. (1991). "Introduction aux lois de comportement des sables très peu denses." *Revue Française de Géotechnique*, 54, 65–73.

Bolton, M. D. (1986). "The strength and dilatancy of sand." *Geotechnique*, 36(1), 65–78.

Fukushima, S., and Tatsuoka, F. (1984). "Strength and deformation characteristics of saturated sand at extremely low pressures." *Soils Found.*, 24(4), 30–48.

Kolymbas, D., and Wu, W. (1990). "Recent results of triaxial tests with granular materials." *Powder Technol.*, 60, 99–119.

Konrad, J.-M., Flavigny, E., and Meghachou, M. (1991). "Comportement non drainé du sable d'Hostun lâche." *Revue Française de Géotechnique*, 54, 53–63.

Lancelot, L., and Shahrour, I. (1994). "Mechanical behaviour of a chemical powder at low stress level: Influence of temperature and humidity." *Powder Handl. Process.*, 6(3), 303–308.

Lo, S.-C. R., and Chu, J. (1993). "One test determination of the failure curve of a granular material by strain path testing." *Soils Found.*, 33(1), 176–181.

Menzies, B. (1988). "A computer controlled hydraulic triaxial testing system." *Advance triaxial testing of soil and rock*, ASTM STP 977, R. T. Donaghe, R. C. Chaney, and M. L. Silver eds., ASTM, Philadelphia, 82–94.

Ponce, V. M., and Bell, J. M. (1971). "Shear strength of sand at extremely low pressures." *J. Soil Mech. and Found. Div.*, 97(4), 625–638.

Roscoe, K. H., Schofield, A. N., and Wroth, C. P. (1958). "On the yielding of soils." *Geotechnique*, 8(1), 22–53.

Rowe, P. W. (1962). "The stress-dilatancy relation for static equilibrium of an assembly of particles in contact." *Proc. R. Soc. London*, 269, 500–527.

Copyright of Journal of Engineering Mechanics is the property of American Society of Civil Engineers and its content may not be copied or emailed to multiple sites or posted to a listserv without the copyright holder's express written permission. However, users may print, download, or email articles for individual use.